

# Construction of $\alpha$ -Helix Peptides with $\beta$ -Cyclodextrin and Dansyl Units and Their Conformational and Molecular Sensing Properties

Sachiko Matsumura,<sup>[a]</sup> Seiji Sakamoto,<sup>[a]</sup> Akihiko Ueno,<sup>\*,[a]</sup> and Hisakazu Mihara<sup>\*,[a, b]</sup>

**Abstract:** In order to apply de novo peptide design to molecular sensing, we designed and synthesized  $\alpha$ -helical peptides with  $\beta$ -cyclodextrin ( $\beta$ -CDx) as a binding site and a dansyl unit (Dns) as a fluorescence sensing site. The conformational and molecular sensing properties of the peptides with  $\beta$ -CDx and Dns in various positions were investigated. Circular dichroism and fluorescence measurements revealed that  $\beta$ -CDx and Dns form intramolecular complexes which depend on their positions in the peptides. In the 17 residual peptides named

EK3 and EK3R, in which  $\beta$ -CDx and Dns were introduced at the fourth and the eighth positions (EK3) or at the eighth and the fourth positions (EK3R), Dns was deeply included in the CDx cavity and formed a more stable self-inclusion complex with CDx than in the peptides EK6 and EK6R, in which these moieties were at the eighth and the

fifteenth positions or at the fifteenth and the eighth positions, respectively. The stability of the self-inclusion complex between  $\beta$ -CDx and Dns controlled the  $\alpha$ -helix structure as well as the binding and sensing abilities for the exogenous guests. These results demonstrate the usefulness of peptide tertiary structure for arranging CDx and other functional units, and suggest that this approach is important in the development of a new type of CDx-based sensory system.

**Keywords:** cyclodextrins • helical structures • inclusion compounds • molecular recognition • peptides

## Introduction

One of the great challenges in chemistry is to produce molecular-recognition devices such as those in proteins, but with smaller molecular structures. Early research has focused on small cyclic molecules such as cyclodextrins, calixarenes, and crown ethers.<sup>[1]</sup> On the other hand, recent advances in de novo peptide and protein design have enabled us to construct various structural and functional motifs.<sup>[2–6]</sup> Nevertheless, it remains difficult to construct a pocket to catch small molecules in defined structures of peptides. To introduce a binding pocket with a simple structure into peptide systems, cyclodextrin (CDx) would be an appropriate compound. Cyclodextrins (CDxs) are cyclic oligosaccharides, mainly composed of six, seven, and eight D-(+)-glucopyranose units for  $\alpha$ -,  $\beta$ -, and  $\gamma$ -CDx, respectively. They are well-known host compounds because of their remarkable ability to include a variety of organic compounds within their hydrophobic

cavities in aqueous solution. The hydrophobic nature and size variability of this cavity have been utilized, for example, as enzyme mimics, models for protein–substrate binding, and solubilizers for water-insoluble substances.<sup>[7]</sup> Furthermore, modified CDxs with a chromophore have been developed as color or fluorescence indicators for various guests.<sup>[8–10]</sup> Some examples of modified CDxs have been demonstrated to allow the selectivity and binding ability to be modulated by means of an environmental unit such as various amino acids.<sup>[10a–c, 11]</sup> For desirable modulation, it is necessary to control the location and orientation of several functional units around the CDxs. It is difficult, however, to control three-dimensional arrangement or orientation of these functional units by using CDx derivatives alone.

In the present study, we provide a new strategy with de novo peptide design in the development of sensory systems using CDxs. An  $\alpha$ -helix structure has been frequently chosen as a secondary structure in the design of functional polypeptides, since the design is well established.<sup>[2, 3, 6, 12, 13]</sup> For example,  $\alpha$ -helical and bundled peptides which showed characteristic structures and/or catalytic activities, have been reported.<sup>[2, 3, 6, 14, 15]</sup> An  $\alpha$ -helical peptide is expected to offer the rigid scaffold for the arrangement of a CDx and other functional units, and also to allow the modification of the ability of the CDx by means of amino acid side chains on peptide secondary structure. In order to explore the capability of  $\alpha$ -helical peptides in CDx-based sensory systems, we

[a] Dr. H. Mihara, Dr. A. Ueno, S. Matsumura, Dr. S. Sakamoto  
Department of Bioengineering  
Faculty of Bioscience and Biotechnology  
Tokyo Institute of Technology, Yokohama 226-8501 (Japan)  
Fax: (+81) 45-924-5833  
E-mail: hmihara@bio.titech.ac.jp

[b] Dr. H. Mihara  
Form and Function, PRESTO  
Japan Science and Technology Corporation (Japan)

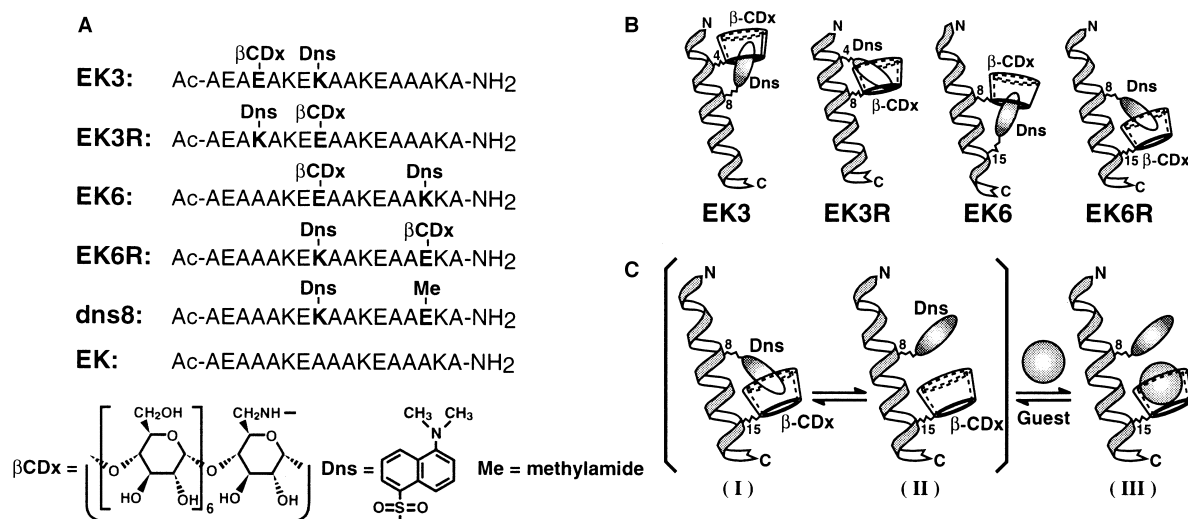
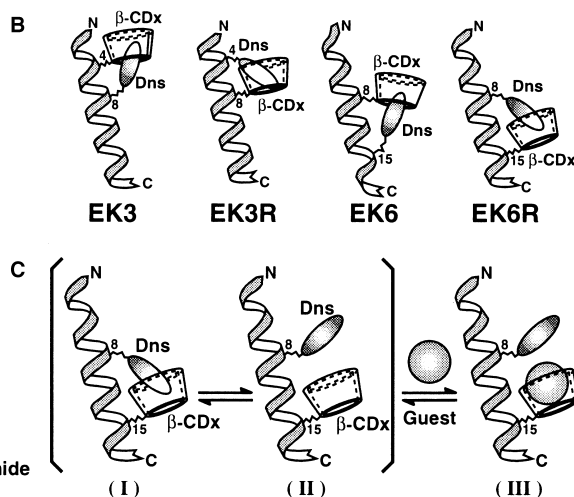


Figure 1. A) Amino acid sequences of the designed peptides; B) helix ribbon diagrams illustrating the positions of  $\beta$ -CDx and Dns in an  $\alpha$ -helix; C) schematic illustration of the equilibrium between intramolecular and intermolecular inclusion complex.

designed and synthesized a variety of  $\alpha$ -helical peptides with a  $\beta$ -CDx as a binding site and a dansyl unit (Dns) as a fluorophore (Figure 1). Dns is a popular fluorescence probe highly sensitive to the polarity of its microenvironment. Although in a polar solvent, such as water, Dns emits weakly, in a nonpolar solvent the group exhibits a stronger emission with a blue shift in fluorescence wavelength. Many studies have reported that the fluorescence emission of dansyl-modified CDxs is made responsive to guest molecules by changing the location from the inside to the outside of the CDx cavity.<sup>[10, 16, 17]</sup> Therefore, Dns can be used as a suitable probe to estimate the binding ability of CDx. We designed and synthesized a series of  $\alpha$ -helix peptides, in which  $\beta$ -CDx and Dns were introduced in different directions or positions, and studied the conformational and molecular-sensing properties by means of UV, circular dichroism (CD), fluorescence, and fluorescence-decay measurements. We report here, for the first time, the utility of the combined systems of CDx, fluorophore, and  $\alpha$ -helical peptide.

#### Abstract in Japanese:

デノボ設計により分子認識能を有するペプチドを構築する試みとして、分子認識部位としてシクロデキストリンを複合化した系について報告する。 $\alpha$ -ヘリックスペプチドの側鎖上に $\beta$ -シクロデキストリンと蛍光性単位としてダンシル基を配置し、ペプチド上でのシクロデキストリンとダンシル基の自己包接錯体形成能とゲスト認識能を調べた。ペプチド立体構造中でシクロデキストリンとダンシル基の導入位置を変えることにより、異なる安定性をもつ自己包接錯体が形成された。両機能性単位間の距離が近いほうが、離れているときと比べ、より安定な包接錯体を形成し、同時に $\alpha$ -ヘリックス構造を安定化した。また自己包接錯体形成能の違いにより、ゲスト認識能もそれぞれ異なった。本研究により、シクロデキストリンと機能性基を空間配置する上での、ペプチド立体構造の有効性が示された。ペプチド立体構造を利用することは、シクロデキストリンを用いた機能性分子の設計に、新たな展開をもたらすだろう。



## Results and Discussion

**Design and synthesis:** For a stable  $\alpha$ -helical peptide for the construction of the CDx–Dns– $\alpha$ -helix hybrids, we selected the 17-residual Ala-based peptide (EK peptide), which was originally designed by Marqusee and Baldwin.<sup>[18]</sup> This peptide has three Glu–Lys pairs to form salt bridges in the side chains of the  $\alpha$ -helical form. We employed another pair of Glu and Lys residues at the fourth and the eighth (EK3, EK3R) or the eighth and the fifteenth (EK6, EK6R) positions in place of Ala residues to combine  $\beta$ -CDx and Dns selectively on the side chains of these residues (Figure 1). Four peptides were designed to examine the effects of the positions and directions of  $\beta$ -CDx and Dns moieties on the  $\alpha$ -helix structure and the molecular-sensing properties. In the peptides of EK3 and EK3R,  $\beta$ -CDx and Dns moieties were introduced at intervals of three residues (ca. one turn of  $\alpha$ -helix), while in the peptides of EK6 and EK6R, both moieties were placed at six residues apart (ca. two turns of  $\alpha$ -helix). In the EK3 and EK6 peptides, the  $\beta$ -CDx moiety was located at the N-terminal side to Dns, whereas in the EK3R and EK6R the order of the moieties was reversed. In all peptides, the N- and C-terminals were converted into acetyl and carboxamide groups, respectively, in order to avoid unfavorable helix-dipole interactions. The peptides were synthesized by the solid-phase method using the Fmoc strategy. To introduce the  $\beta$ -CDx and Dns moieties at the specific positions, the Glu and Lys residues which were to remain intact were protected by Bzl and ClZ groups, respectively. After the peptide synthesis, Dns-Cl was coupled with the  $\epsilon$ -amino group of the Lys side chain, and then the 6-NH<sub>2</sub>- $\beta$ -CDx was coupled with the carboxy group of the Glu side chain. The peptides were purified with reversed-phase HPLC, and identified by matrix-assisted laser desorption/ionization time-of-flight mass spectrometry (MALDI-TOFMS) and amino acid analysis.

**Circular dichroism study:** All peptides designed in this study exhibited far-ultraviolet circular dichroism (CD) spectra

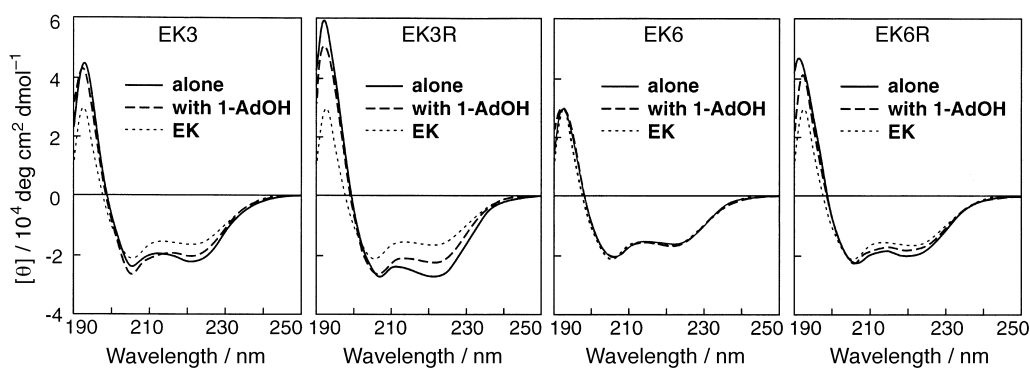


Figure 2. CD spectra at the amide region of the designed peptides alone and in the presence of 1-adamantanol (1-AdOH) in Tris·HCl buffer (20 mM, pH 7.4) at 25 °C. [Peptide] = 20  $\mu$ M. [1-AdOH] = 3.0 mM.

characteristic of  $\alpha$ -helical conformations in Tris·HCl buffer (20 mM, pH 7.4) at 25 °C (Figure 2). Table 1 summarizes the molar ellipticities at 222 nm ( $[\theta]_{222}$ ) and  $\alpha$ -helix contents

Table 1. Molar ellipticities and  $\alpha$ -helix contents of the designed peptides alone and in the presence of 1-adamantanol (1-AdOH) in the buffer (pH 7.4) at 25 °C.

	Guest	EK3	EK3R	EK6	EK6R	EK
$[\theta]_{222}$ <sup>[a]</sup>	–	–21 800	–26 600	–15 600	–19 000	–16 100
	1-AdOH <sup>[b]</sup>	–19 900	–19 700	–16 100	–17 100	–16 400
$\alpha$ -helix content [%]	–	61	75	44	53	45
	1-AdOH <sup>[b]</sup>	56	55	45	48	46

[a] deg cm<sup>2</sup> dmol<sup>–1</sup>. [b] [1-AdOH] = 3.0 mM.

estimated from  $[\theta]_{222}$  for the peptides.<sup>[19]</sup> The order of helix formation was EK3R (75%) > EK3 (61%) > EK6R (53%) > EK6 (44%), that is, EK3R, EK3, and EK6R formed more helical structures than the original EK peptide (45%). The difference in the helical propensity of the peptides was not the result of aggregation, as judged by the mobility on the gel filtration column and the concentration independence of  $[\theta]_{222}$  in the range of 5–100  $\mu$ M. At a higher concentration, however, intermolecular events may not be ignored, though the original peptide EK is known to be monomeric in solution.<sup>[18]</sup> In the cases of EK3R, EK3, and EK6R, the addition of 1-adamantanol (1-AdOH) as a high-affinity exogenous guest for  $\beta$ -CDx,<sup>[9, 10, 20]</sup> reduced the helix contents to 55%, 56%, and 48%, respectively (Figure 2, Table 1). These results suggest that  $\beta$ -CDx and Dns formed intramolecular inclusion complexes and that the complexation caused higher helical structures.

Insight into the self-inclusion of the Dns into the  $\beta$ -CDx cavity was provided from the CD spectra in the absorption region of the Dns, by taking advantage of the fact that an achiral molecule included in the chiral CDx cavity may exhibit an induced circular dichroism (ICD) in its absorption region.<sup>[16, 21–23]</sup> In the absence of a guest, EK3 and EK6 showed similar patterns of ICD spectra, and those of EK3R and EK6R also resembled each other (Figure 3). EK3 and EK6 had a negative ICD band near 340 nm and a positive band near 260 nm. This observation was consistent with the axial complexation between  $\beta$ -CDx and Dns,<sup>[16, 22, 23]</sup> that is, with the long axis of naphthalene parallel to the  $\beta$ -CDx axis. On the contrary, EK3R and EK6R showed the opposite signs

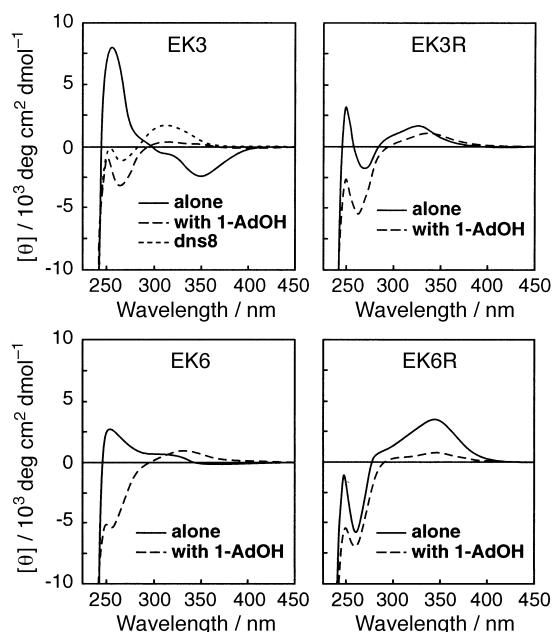


Figure 3. CD spectra at the Dns absorption region of the designed peptides alone and in the presence of 1-adamantanol (1-AdOH) in Tris·HCl buffer (20 mM, pH 7.4) at 25 °C. [Peptide] = 30–50  $\mu$ M. [1-AdOH] = 2.0 mM.

of ICD spectra as expected for the equatorial complexation.<sup>[22, 23]</sup> Although the  $\beta$ -CDx–Dns distances of EK3 and EK6 are the same as EK3R and EK6R, respectively, the order of these moieties is not the same:  $\beta$ -CDx is located at an N-terminal side to Dns in EK3 and EK6, whereas this order is reversed in EK3R and EK6R. A possible explanation for the different complex structures implied from the ICD spectra is that  $\beta$ -CDx is directed in a defined manner so that the  $\beta$ -CDx and Dns moieties interact in different ways. One possibility to explain the  $\beta$ -CDx direction is the dipole-to-dipole interaction between the  $\beta$ -CDx and an  $\alpha$ -helix. The dipole moment of an  $\alpha$ -helix is directed from the C-terminus to the N-terminus,<sup>[13a,b]</sup> and  $\beta$ -CDx also has a dipole moment directed from the secondary hydroxy side (the wider side) toward the primary (narrower) side.<sup>[24]</sup> On this basis, the moments of the  $\beta$ -CDx and  $\alpha$ -helix are antiparallel and consequently Dns is inserted into the  $\beta$ -CDx cavity from the narrower side in the peptides EK3 and EK6 (Figure 1). The observed ICD, which suggests the axial complexation, was compatible with the modification

of the  $\beta$ -CDx at C(6) (at the narrower side) by the Dns moiety.<sup>[16]</sup> In the cases of EK3R and EK6R, Dns would be at the wider side of the  $\beta$ -CDx and therefore allows the equatorial complexation. Upon the addition of 1-AdOH, the ICD spectra of all peptides changed to a common pattern similar to that of the reference peptide, dns8 (with Dns only at the eighth position), with a slight positive ICD band near 340 nm and a negative one near 260 nm (Figure 3).

**Fluorescence study:** The fluorescence spectra of Dns in the peptides also confirmed the intramolecular inclusion complexation of  $\beta$ -CDx and Dns by the fact that EK3, EK3R, EK6, and EK6R emitted much more strongly than dns8 (Figure 4), suggesting that the Dns moiety is located in a hydrophobic environment.<sup>[25]</sup> Furthermore, the fluorescence intensities decreased remarkably and the peak maxima shifted to longer wavelength upon the addition of ursodeoxycholic acid (UDCA) as a guest. This guest-induced fluorescence variation indicates that the Dns moiety is excluded from the cavity of  $\beta$ -CDx toward the bulk water environment as the guest is accommodated. The order of the maximum intensities was EK3R > EK3 > EK6R > EK6 and their maximum wavelengths were 524 nm, 534 nm, 529 nm, and 540 nm, respectively, in the absence of the guest. These data reflect the different polarity around the Dns moiety in the peptides. The Dns moiety of EK3R and EK6R is located at the N-terminal side from  $\beta$ -CDx and accordingly exhibits stronger fluorescence at shorter wavelength than EK3 and EK6, in which the Dns moiety is located at the C-terminal side from  $\beta$ -CDx. These results indicate that the Dns moiety of EK3R or EK6R is located in a more hydrophobic environment or more deeply included into the cavity of  $\beta$ -CDx than for EK3 or EK6, respectively. If the deeper inclusion of the Dns in the EK3R and EK6R is made possible by its insertion from the wider side of  $\beta$ -CDx, these results appear to support the complexation model assumed from the ICD spectra (Figure 1). Furthermore, the order of the fluorescence intensity is the same as that of  $\alpha$ -helicity, indicating that the  $\beta$ -CDx–Dns complexation tends to stabilize the  $\alpha$ -helix structure.

Time-resolved fluorescence experiments are expected to provide useful information about the environment around Dns in the peptides. It is known that the lifetime of the fluorescence guest included within the  $\beta$ -CDx is longer than that outside the  $\beta$ -CDx cavity.<sup>[26]</sup> In the case of dansyl-modified  $\beta$ -CDxs, it has also been reported that they have two components with fluorescence lifetimes of approximately 17 ns and 6 ns, associated with the Dns moiety inside and outside the cavity, respectively.<sup>[10c, 16, 17]</sup> The lifetime measurements of EK3, EK3R, EK6, and EK6R revealed that they have two lifetimes: the longer one (19–21 ns), which was absent in the case of dns8, and the shorter one (4–8 ns), which was similar to the lifetime of the main fraction of dns8 (4.2 ns) (Table 2). The data suggest that the Dns moiety exists in an

Table 2. Fluorescence lifetimes ( $\tau$ ) and molar fractions ( $\alpha$ ) for the designed peptides alone and in the presence of 1-adamantanol (1-AdOH) in the buffer (pH 7.4) at 25 °C.<sup>[a]</sup>

Peptide	Guest	$\tau_1$ [ns]	$\alpha_1$	$\tau_2$ [ns]	$\alpha_2$
EK3		18.8	0.850	4.4	0.150
EK3	1-AdOH <sup>[b]</sup>	14.7	0.568	5.2	0.432
EK3R		20.6	0.908	8.5	0.092
EK3R	1-AdOH <sup>[b]</sup>	15.4	0.668	5.3	0.332
EK6		18.6	0.574	4.8	0.426
EK6	1-AdOH <sup>[b]</sup>	11.2	0.256	4.3	0.744
EK6R		18.8	0.723	6.4	0.277
EK6R	1-AdOH <sup>[b]</sup>	13.8	0.345	5.0	0.655
dns8		4.2	0.894	1.6	0.106

[a] Data refer to the best-fitting model for each compound ( $\chi^2 < 1.2$ ). [b] [1-AdOH] = 4.7 mM.

equilibrium between two conformations, located inside and outside the cavity for longer and shorter lifetime species, respectively (Figure 1C). It is rather strange that dns8 has two lifetimes of 4.2 ns (89%) and 1.6 ns (11%) in spite of the absence of a CDx unit. The lifetime of the main fraction (4.2 ns) was compatible with the Dns moiety exposed to bulk water. However, the origin of the shorter one (1.6 ns) is not clear. It might be produced as the result of quenching by a proximal Lys side chain.

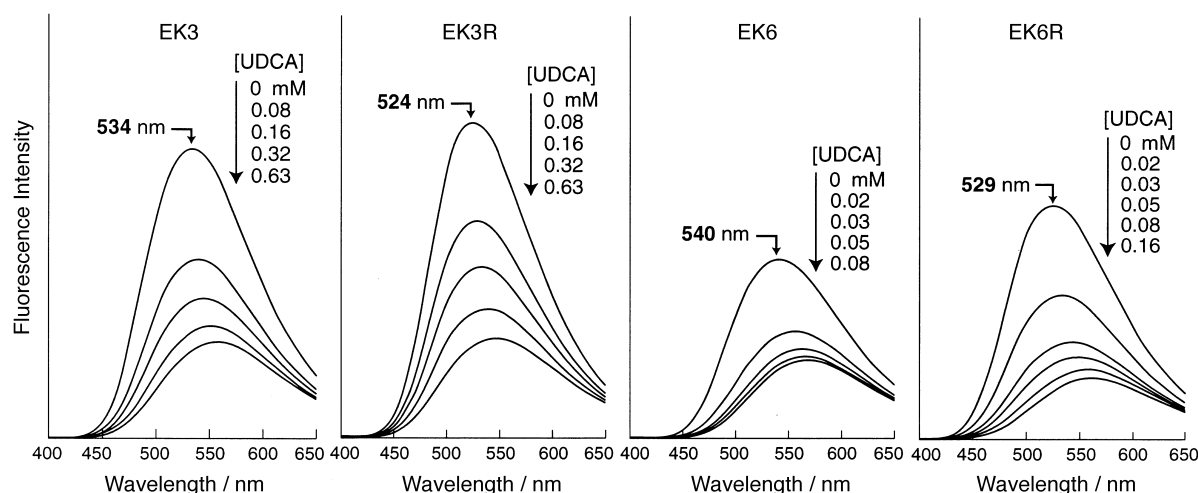


Figure 4. Fluorescence emission spectra of the peptides alone and in the presence of various concentrations of ursodeoxycholic acid (UDCA) in Tris · HCl buffer (20 mM, pH 7.4) at 25 °C. [Peptide] = 16  $\mu$ M.

The preexponential factor ( $\alpha_i$ ) for each component represents the population of Dns in the corresponding environment.<sup>[17, 27]</sup> EK3R and EK6R have larger molar fractions of long-lived components (EK3R, 0.91; EK6R, 0.72) than EK3 and EK6 (EK3, 0.85; EK6, 0.57), respectively (Table 2). It is obvious that the self-inclusion forms in EK3R and EK6R are more favorable than EK3 and EK6, respectively. Another factor that affects the ratio of self-complexation is the distance between the  $\beta$ -CDx and Dns, and the shorter interval in EK3 and EK3R (ca. one turn of  $\alpha$ -helix) was better than the longer interval in EK6 and EK6R (ca. two turns of  $\alpha$ -helix). The result is consistent with the fluorescence intensities of these peptides (Figure 4). Furthermore, the addition of 1-AdOH increased the fraction of shorter lifetime component in the peptides but decreased the fraction of the longer lived one. All these results are consistent, and support the exclusion of Dns from inside the cavity upon the guest binding.

**Stability of complex and peptide:** It was shown that the peptides used in this study form  $\alpha$ -helices with different helix content and that the addition of guests decreases the  $\alpha$ -helicities in some peptides (Table 1). Since complexation between  $\beta$ -CDx and Dns appears to affect the peptide secondary structure, the stabilities of  $\beta$ -CDx–Dns complexes and peptides were estimated by thermal denaturation studies, and the relationship between the two factors has been explored.

In order to evaluate the stability of the  $\beta$ -CDx–Dns complex, fluorescence-decay analyses at six different temperatures from 10 to 60 °C were carried out. The equilibrium constants ( $K$ ) between two conformations, with the Dns moiety inside and outside the cavity, were estimated at each temperature. The results afforded linear relationships on the van't Hoff plots of  $\ln K$  versus  $T^{-1}$ . Then, the Gibbs free energy change for the formation of the  $\beta$ -CDx–Dns complex in each peptide was estimated (Table 3). It was revealed that the order of the stabilities was EK3R > EK3 > EK6R > EK6, which is in agreement with the order of fluorescence intensities, that is, peptides with Dns in a more hydrophobic environment of  $\beta$ -CDx have more stable  $\beta$ -CDx–Dns complexes, probably, affording more stable  $\alpha$ -helix.

Table 3. The stabilities of  $\beta$ -CDx–Dns complexes and peptides at 25 °C and melting temperatures of the peptides.

	EK3	EK3R	EK6	EK6R	EK
Fluorescence lifetime measurement					
$\Delta G$ [kJ mol <sup>-1</sup> ]	-4.30	-5.68	-0.59	-2.52	-
Circular dichroism measurement					
$\Delta G$ [kJ mol <sup>-1</sup> ]	-0.41	-2.53	1.11	-0.46	0.47
$\Delta\Delta G$ [kJ mol <sup>-1</sup> ]	-0.88	-3.00	0.64	-0.93	-
$T_m$ [°C]	28	44	17	28	22
$\Delta T_m$ [°C]	6	22	-5	6	-

On the other hand, the thermal stability of the peptide was examined by CD measurements. As the temperature of the peptide solution increased, the spectra characteristic of an  $\alpha$ -helical form gradually transformed into relatively featureless spectra of an unfolded form at approximately 90 °C. The

presence of an isodichroic point at 202 nm is consistent with the helix-coil transition occurring at this temperature range. The analyses of the thermal denaturation curves at 222 nm afforded linear van't Hoff plots and  $\Delta G$  for the peptides were then estimated (Table 3). Each peptide has its own stability, as expected, and the introduction of a  $\beta$ -CDx–Dns complex into the peptide appears to contribute to the stability of the  $\alpha$ -helical conformation. The peptide stabilities (EK3R > EK3 = EK6R > EK6) are almost comparable with the  $\beta$ -CDx–Dns complex stabilities. This observation was in accord with the facts that the order of the stabilities of the  $\beta$ -CDx–Dns complex was the same as the order of the  $\alpha$ -helix contents (EK3R > EK3 > EK6R > EK6) (Table 1) and that the  $\alpha$ -helicity was reduced with decomposition of the complex by the addition of an exogenous guest. Particularly in the case of EK3R, which has the most stable  $\beta$ -CDx–Dns complex, the melting temperature of the peptide dramatically increased by 22 °C as compared with that of the EK peptide. The peptide stabilities, however, are not completely parallel to the  $\beta$ -CDx–Dns complex stabilities. This might mean that complicated factors, including water molecules, affect the  $\alpha$ -helix stability.<sup>[28]</sup> Moreover, the  $\alpha$ -helical stability of EK3R and EK6R was larger than that of EK3 and EK6, respectively. These results are also comparable with those of the fluorescence studies, suggesting that the different direction of insertion of Dns into the  $\beta$ -CDx cavity causes variation in the  $\alpha$ -helix structure.

**Molecule sensing properties:** The fluorescence intensities of EK3, EK3R, EK6, and EK6R decreased upon the addition of a guest (Figure 4), which indicated that these peptides might have guest-sensing abilities similar to fluorophore-appended  $\beta$ -CDxs.<sup>[8–10]</sup> Therefore, the sensing properties for guest molecules (Figure 5) were examined by using the fluorescence spectra of the Dns-incorporated peptides. The UV absorption spectra of the peptides were slightly shifted (337–330 nm) to shorter wavelengths upon addition of guest molecules such as 1-AdOH with an isosbestic point at approximately 340 nm.

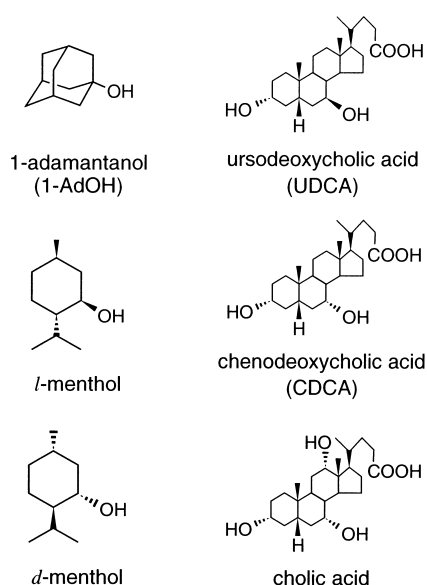


Figure 5. The structures of guest compounds.

The fluorescence spectra were measured by excitation at the wavelength of the isosbestic point, and we observed that the fluorescence intensity decreased remarkably; the peak maximum is shifted to longer wavelengths upon addition of UDCA as a guest. Similar phenomena were observed for all guest compounds used in this study.

The binding constants ( $K_b$ ) of the peptides (host) for various guests were evaluated by using the fluorescence intensity variation  $\Delta I/I_0$ , where  $\Delta I = I_0 - I$ , and  $I_0$  and  $I$  were the fluorescence intensities in the absence and presence of the guest, respectively, measured at the maximum-emission wavelength of the peptides alone. The  $\Delta I/I_0$  values, obtained at different guest concentrations, were fitted to the equation for a 1:1 host-guest complex formation.<sup>[9, 10]</sup>

The binding constants of the peptides for various guests are shown in Table 4. The binding constants for 1-AdOH were

Table 4. The binding constants ( $K_b$ ) and guest-induced emission variations ( $\Delta I_{max}/I_0$ ) of the designed peptides for various guests in the buffer (pH 7.4).

Guests	EK3	EK3R	EK6	EK6R
	$K_b [10^3 M^{-1}]$ ( $\Delta I_{max}/I_0$ )	$K_b [10^3 M^{-1}]$ ( $\Delta I_{max}/I_0$ )	$K_b [10^3 M^{-1}]$ ( $\Delta I_{max}/I_0$ )	$K_b [10^3 M^{-1}]$ ( $\Delta I_{max}/I_0$ )
1-adamantanol	4.93 (0.435)	2.19 (0.579)	18.9 (0.579)	13.0 (0.691)
<i>l</i> -menthol	0.413 (0.456)	0.411 (0.462)	2.85 (0.627)	1.46 (0.734)
<i>d</i> -menthol	0.343 (0.529)	0.307 (0.499)	2.78 (0.633)	1.40 (0.733)
ursodeoxycholic acid	12.1 (0.812)	7.28 (0.881)	236 (0.673)	154 (0.831)
chenodeoxycholic acid	3.11 (0.775)	1.90 (0.871)	45.0 (0.665)	27.6 (0.826)
cholic acid	n.d. <sup>[a]</sup> (n.d.) <sup>[a]</sup>	n.d. <sup>[a]</sup> (n.d.) <sup>[a]</sup>	0.644 (0.743)	0.625 (0.786)

[a] n.d. = not determined. The value could not be determined due to the small change in the spectrum.

larger than those for *l*-menthol and *d*-menthol. Among the steroids, binding constants for ursodeoxycholic acid (UDCA) and chenodeoxycholic acid (CDCA) with two hydroxy groups were larger than the binding constants for cholic acid with three hydroxy groups. These properties were in common with chromophore-modified  $\beta$ -CDx derivatives,<sup>[9, 10]</sup> and confirmed that the binding site works in these peptide systems and the guest-selectivity of  $\beta$ -CDx is not disturbed by the peptide scaffold.

Each peptide showed characteristic binding constants for all guests examined, and the order was EK6 > EK6R > EK3 > EK3R. This order is the reverse of the order of the complex-stabilities between  $\beta$ -CDx and Dns, and suggests that the formation of tight intramolecular complexes was not suitable for the intermolecular complexation with exogenous guests. EK6 and EK6R show larger binding constants for the guests, especially for the steroids (20-fold higher), compared with EK3 and EK3R. These results indicate that the binding property of the  $\beta$ -CDx-peptides is correlated to the distance between the  $\beta$ -CDx and Dns moieties. The  $\beta$ -CDx moiety in EK6 and EK6R, which is six residues apart from Dns, is more highly accessible to various guests than that in EK3 and EK3R. It should be noted that the binding constants of EK6

and EK6R are comparable with those of dansyl-modified  $\beta$ -CDxs.<sup>[10]</sup>

The sensitivity factors of the peptides for various guests were evaluated using fluorescence-intensity variation  $\Delta I/I_0$  at a guest concentration of 100  $\mu$ M (peptide concentration of 10  $\mu$ M). The values of  $\Delta I/I_0$  are correlated to the binding constants, and EK6 and EK6R are more sensitive than EK3 and EK3R to each of the guests (Figure 6). These differences observed in the binding and sensing behavior suggest that the molecular recognition and sensing abilities can be controlled by the arrangement of CDx and Dns moieties.

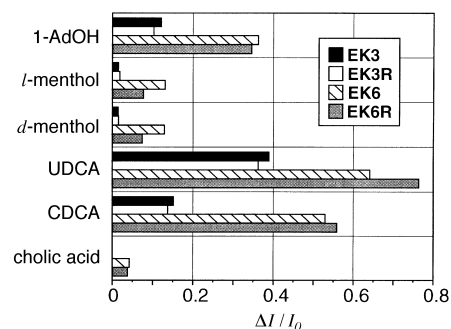


Figure 6. The sensitivity factors of the designed peptides (10  $\mu$ M) for various guests (100  $\mu$ M) from the variation of fluorescence intensity in Tris-HCl buffer (20 mM, pH 7.4) at 25  $^{\circ}$ C.

Additionally, in order to know the effect of rigid  $\alpha$ -helix conformation on the sensing property, denaturation studies of peptide conformation were carried out using guanidine hydrochloride (GuHCl) (Figure 7). The  $\alpha$ -helix conformation

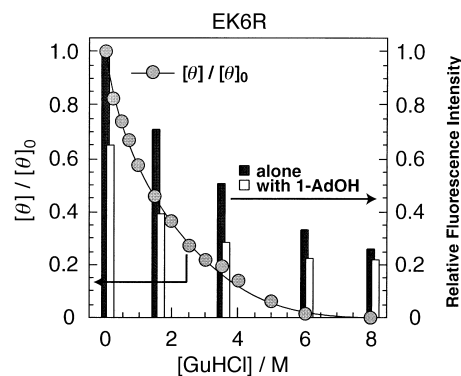


Figure 7. The effect of  $\alpha$ -helical structure on the sensing ability estimated by the denaturation study using guanidine hydrochloride (GuHCl).  $[\theta]/[\theta]_0$  is the ratio of molar ellipticity at 222 nm at the indicated molarity of GuHCl to the ellipticity without GuHCl. The relative fluorescence intensity of the designed peptides (10  $\mu$ M) alone and in the presence of 1-adamantanol (1-AdOH; 100  $\mu$ M) in 20 mM Tris-HCl buffer (pH 7.4) at 25  $^{\circ}$ C is also plotted.

of EK6R was gradually unfolded with the addition of GuHCl. In response to this unfolding, the fluorescence intensity of Dns decreased in the presence and absence of 1-AdOH. Sensitivity to the guest molecule ( $\Delta I/I_0$ ) also diminished in response to the decay of the peptide secondary structure. These results demonstrate that the  $\alpha$ -helix structure plays an important role for complex formation between  $\beta$ -CDx and Dns.

## Conclusion

The molecule binding moiety ( $\beta$ -CDx) and the fluorescence moiety (Dns) were deployed on the rigid  $\alpha$ -helix scaffold of peptides in various directions or positions. The formation of the complex between  $\beta$ -CDx and Dns was controlled by their positioning, which can be regulated by peptide design. The complexation between  $\beta$ -CDx and Dns in each peptide has been shown to control not only the binding and sensing abilities for the exogenous guests but also the  $\alpha$ -helix structure. The peptide with a highly stable self-inclusion complex prefers to take a higher  $\alpha$ -helix form. With respect to the sensing property for the exogenous guests, however, such tight self-inclusion complexation is not preferable and the sensing ability depends on the distance between  $\beta$ -CDx and Dns. The behavior of the designed peptides was generated by the control of the locations of functional units by use of the peptide structure, and demonstrate that the peptide is useful for the arrangement of the CDx and other functional units three-dimensionally and the modulation of the binding ability of CDx. Application of the peptide scaffold to the CDx-based molecular sensor will lead to a new field of molecular recognition and sensing with CDx, since a variety of amino acid side chains can be utilized for functionalization. The conjugation of CDx to the peptide is beneficial to the de novo approach for designing functional peptides, because construction of the well-defined binding moiety can be easily accomplished with a CDx moiety. This approach will be effective in the design of a new type of peptide with extraordinary abilities as sensors and/or artificial enzymes.

## Experimental Section

**Materials and methods:** All chemicals and solvents were of reagent or HPLC grade. Amino acid derivatives and reagents for peptide synthesis were purchased from Watanabe Chemical Co. (Hiroshima, Japan).  $\beta$ -Cyclodextrin ( $\beta$ -CDx) was kindly donated by Nihon Shokuhin Kako Co., Ltd., and was used as received. Mono-6-deoxy-6-amino- $\beta$ -cyclodextrin ( $\text{NH}_2$ - $\beta$ -CDx) was prepared as previously reported.<sup>[9c]</sup> All the guest compounds were purchased from Tokyo Kasei and were used without further purification. All peptides were synthesized manually by the solid-phase method using the Fmoc-strategy.<sup>[29]</sup> The peptides were purified by reversed-phase HPLC. HPLC was carried out on a Wakosil 5C18 column (Wako Pure Chemical Industries) (4.6  $\times$  150 mm) or a YMC ODS A-323 column (YMC Co.) (10  $\times$  250 mm) by employing a Hitachi L-7000 HPLC system. The peptides were identified by MALDI-TOFMS. MALDI-TOF mass spectra were measured on a Shimadzu KOMPACT MALDI III mass spectrometer with 3,5-dimethoxy-4-hydroxycinnamic acid or 2,5-dihydroxybenzoic acid as a matrix. Amino acid analysis was carried out after hydrolysis in 6.0 M HCl at 110 °C for 24 h in a sealed tube. The peptide concentration was determined by quantitative amino acid analysis with valine as internal standard.

**Peptide synthesis:** Peptides were synthesized manually by stepwise elongation of Fmoc-amino acids on a Rink amide resin<sup>[30]</sup> according to a reported procedure with Fmoc-AA [Fmoc-Ala  $\cdot$  H<sub>2</sub>O, Fmoc-Glu(OBzl), Fmoc-Glu(O $t$ Bu)  $\cdot$  H<sub>2</sub>O, Fmoc-Lys(Boc), Fmoc-Lys(CIZ); Bzl, benzyl;  $t$ Bu, *tert*-butyl; Boc, *tert*-butyloxycarbonyl; ClZ, 2-chloro-carbobenzoxy], benzotriazol-1-yloxytris(dimethylamino) phosphonium hexafluorophosphate (BOP), and 1-hydroxybenzotriazole hydrate (HOBt  $\cdot$  H<sub>2</sub>O). The Lys and Glu residues coupled with dansyl chloride and  $\text{NH}_2$ - $\beta$ -CDx were protected with Boc and  $t$ Bu, respectively, and the other Lys and Glu residues were with ClZ and Bzl. Coupling efficiency was checked by the Kaiser test.<sup>[31]</sup> To synthesize Ac-peptide resin, the Fmoc-deprotected peptide resin was

treated with acetic anhydride (10 equiv) in 1-methylpyrrolid-2-one (NMP) for 20 min. To remove the resin and protecting groups except for the Bzl and ClZ groups, the peptide resin was stirred in TFA (10 mL) in the presence of *m*-cresol (0.5 mL) as scavenger for 1 h at 25 °C. All crude peptides were identified from the molecular ion peak  $[M + \text{Na}]^+$  in the MALDI-TOF mass spectra.

To introduce dansyl (Dns) group to the deprotected Lys side chain on the crude peptides, dansyl chloride (2 equiv) was added to the crude peptides in DMF in the presence of di-2-propylethylamine (4 equiv), and stirred at 4 °C for 5–6 h. Then,  $\text{NH}_2$ - $\beta$ -CDx (3 equiv), HOBt  $\cdot$  H<sub>2</sub>O (3 equiv) and 1-ethyl-3-(3-dimethylaminopropyl)carbodiimide hydrochloride (3 equiv) were added to the reaction mixtures and allowed to react for two days. Each coupling step was monitored by analytical HPLC and coupling products were identified by MALDI-TOFMS.

To remove Bzl and ClZ groups in the peptides, the peptides were treated with 1 M trimethylsilyl trifluoromethanesulfonate/thioanisole (molar ratios 1:1) in TFA in the presence of *m*-cresol at 0 °C for 1.5 h.<sup>[32]</sup> The peptides were purified by HPLC with a YMC ODS A-323 column, and identified by MALDI-TOFMS and amino acid analysis.

EK3 (total yield from AA-Resin, 17%), EK3R (19%), EK6 (10%) and EK6R (24%); MALDI-TOFMS found  $[M + \text{Na}]^+$  (calcd  $[M + \text{Na}]^+$ ); EK3, 3100.7 (3100.3); EK3R, 3101.0 (3100.3); EK6, 3100.0 (3100.3); EK6R, 3099.6 (3100.3); amino acid analysis of peptides gave satisfactory results.

**CD measurements:** CD spectra were recorded on a J-720WI spectropolarimeter equipped with a thermoregulator with a quartz cell with 0.1 cm pathlength at amide region (190–250 nm) and 1.0 cm at the absorption region of the Dns groups (250–450 nm), respectively. All peptides were dissolved in Tris  $\cdot$  HCl buffer (20 mM, pH 7.4) at a peptide concentration of 20–40  $\mu$ M.

**UV/Vis measurements:** UV/Vis spectra were recorded on a Shimadzu UV-3100 spectrophotometer with a quartz cell with 1.0 cm pathlength. All peptides were dissolved in Tris  $\cdot$  HCl buffer (20 mM, pH 7.4) at a peptide concentration of 20  $\mu$ M.

**Fluorescence measurements:** Fluorescence emission spectra were measured on a Hitachi 850 fluorescence spectrometer with a 1.0  $\times$  1.0 cm quartz cell at 25 °C. All peptides were dissolved in Tris  $\cdot$  HCl buffer (20 mM, pH 7.4) at a peptide concentration of 10  $\mu$ M or 5  $\mu$ M and were excited at an isosbestic point around 340 nm. Fluorescence decay was measured by a time-correlated single-photon counting method on a Horiba NAES-550 system. A self-oscillating flash lamp filled with H<sub>2</sub> was used as a light source. The excitation beam was passed through the filter P/N:340 (Audover Co.), and the emission beam was through the filter Y-44 (Toshiba). Lifetime was obtained by the deconvolution with a nonlinear least-square fitting procedure. All peptides were dissolved in Tris  $\cdot$  HCl buffer (20 mM, pH 7.4) at a peptide concentration of 30–40  $\mu$ M.

**Thermal denaturation:** Each peptide solution [10  $\mu$ M in 20 mM Tris  $\cdot$  HCl buffer, pH 7.4] was loaded into a quartz cell with 0.2 cm pathlength and the CD spectrum was scanned at different temperatures. Spectra were measured at every 5 °C (from 0 to 100 °C) allowing 2 min for equilibration. Unfolding transitions were followed by plotting the ellipticity at 222 nm as a function of temperature. The enthalpy ( $\Delta H$ ) and entropy ( $\Delta S$ ) were examined by plotting  $\ln K$  versus  $T^{-1}$  and the Gibbs free energy ( $\Delta G$ ) was obtained from Equations (1) and (2). In Equation (1)  $K$  is the equilibrium constant and  $[\theta]_{\text{coil}} = [\theta]_{\text{obs}}$  at the high-temperature plateau and  $[\theta]_{\text{helix}} = -35600$ <sup>[19]</sup> and in Equation (2)  $T = 298 \text{ K}^{-1}$ .

$$K = [\text{helix}]/[\text{coil}] = ([\theta]_{\text{obs}} - [\theta]_{\text{coil}})/([\theta]_{\text{helix}} - [\theta]_{\text{obs}}) \quad (1)$$

$$\Delta G = \Delta H - T\Delta S \quad (2)$$

Fluorescence decay was measured at every 10 °C (from 10 to 60 °C) allowing 10 min for equilibration with peptide concentration of 40  $\mu$ M. In this case, the equilibrium constant  $K = \alpha_1/\alpha_2$ , where  $\alpha_1$  is the molar fraction of the long-lived component and  $\alpha_2$  is that of the shorter one.

**Determination of binding constant for  $\beta$ -CDx–guest complex:**  $\beta$ -CDx (in the peptide) in Tris  $\cdot$  HCl buffer (20 mM, pH 7.4) was titrated with guest in increments of about 0.2 equiv ( $\beta$ -CDx concentration of 5  $\mu$ M, guest stock concentration of 200 mM and 40 mM). After each addition of guest, fluorescence emission spectra (400–650 nm) were measured at 25 °C excited at an isosbestic point around 340 nm. The decrease of the intensity

at the maximum emission wavelength of the peptide alone with increasing guest concentration was corrected for dilution and fitted by a single site binding Equation (3) using Kaleida Graph (Synergy Software) where  $H_0$  and  $G_0$  represent the initial concentration of  $\beta$ -CDx (in the peptide) and guest, respectively.

$$\Delta I/I_0 = \{(\Delta I_{\max}/I_0)/2H_0\}[(H_0+G_0+1/K_b) - \{(H_0+G_0+1/K_b)^2 - 4H_0G_0\}^{1/2}] \quad (3)$$

$\Delta I$  denotes the difference in the fluorescence intensity between  $\beta$ -CDx in the absence ( $I_0$ ) and the presence of guest at each concentration ( $I$ ). When all the  $\beta$ -CDxs form the complex,  $\Delta I$  is equal to  $\Delta I_{\max}$ .

- [1] *Comprehensive Supramolecular Chemistry, Vol. 1* (Eds.: J. L. Atwood, J. E. D. Davies, D. D. MacNicol, F. Vögtle, G. W. Gokel), Pergamon, Oxford, **1996**.
- [2] a) J. W. Bryson, S. F. Betz, H. S. Lu, D. J. Suich, H. X. Zhou, K. T. O'Neill, W. F. DeGrado, *Science* **1995**, *270*, 935–941; b) S. F. Betz, J. W. Bryson, W. F. DeGrado, *Curr. Opin. Struct. Biol.* **1995**, *5*, 457–463.
- [3] a) L. Brive, G. T. Dolphin, L. Baltzer, *J. Am. Chem. Soc.* **1997**, *119*, 8598–8607; b) L. Baltzer, *Curr. Opin. Struct. Biol.* **1998**, *8*, 466–470; c) L. Baltzer, K. S. Broo, *Biopolymers* **1998**, *47*, 31–40.
- [4] a) G. K. Walkup, B. Imperiali, *J. Am. Chem. Soc.* **1997**, *119*, 3443–3450; b) M. D. Struthers, R. P. Cheng, B. Imperiali, *Science* **1996**, *271*, 342–345.
- [5] a) M. Engels, D. Bashford, M. R. Ghadiri, *J. Am. Chem. Soc.* **1995**, *117*, 9151–9158; b) M. R. Ghadiri, J. R. Granja, L. K. Buehler, *Nature (London)* **1994**, *369*, 301–304.
- [6] J. P. Schneider, J. W. Kelly, *Chem. Rev.* **1995**, *95*, 2169–2187.
- [7] a) *Comprehensive Supramolecular Chemistry, Vol. 3* (Eds.: J. L. Atwood, J. E. D. Davies, D. D. MacNicol, F. Vögtle, J. Szejtli, T. Osa), Pergamon, Oxford, **1996**; b) R. Breslow, S. D. Dong, *Chem. Rev.* **1998**, *98*, 1997–2011; c) A. R. Hedges, *Chem. Rev.* **1998**, *98*, 2035–2044; d) M. L. Bender, M. Komiya, *Cyclodextrin Chemistry*, Springer, Berlin, **1978**.
- [8] A. Ueno in *Fluorescent Chemosensors for Ion and Molecule Recognition* (Ed.: A. W. Czarnick), ACS Symposium Series 538, American Chemical Society, Washington, DC, **1993**, pp. 74–84.
- [9] a) A. Ueno, T. Kuwabara, A. Nakamura, F. Toda, *Nature (London)* **1992**, *356*, 136–137; b) T. Aoyagi, A. Nakamura, H. Ikeda, T. Ikeda, H. Mihara, A. Ueno, *Anal. Chem.* **1997**, *69*, 659–663; c) K. Hamasaki, H. Ikeda, A. Nakamura, A. Ueno, F. Toda, I. Suzuki, T. Osa, *J. Am. Chem. Soc.* **1993**, *115*, 5035–5040.
- [10] a) A. Ueno, A. Ikeda, H. Ikeda, T. Ikeda, F. Toda, *J. Org. Chem.* **1999**, *64*, 382–387; b) M. Nakamura, A. Ikeda, N. Ise, T. Ikeda, H. Ikeda, F. Toda, A. Ueno, *J. Chem. Soc. Chem. Commun.* **1995**, 721–722; c) H. Ikeda, M. Nakamura, N. Ise, N. Oguma, A. Nakamura, T. Ikeda, F. Toda, A. Ueno, *J. Am. Chem. Soc.* **1996**, *118*, 10980–10988; d) Y. Wang, T. Ikeda, H. Ikeda, A. Ueno, F. Toda, *Bull. Chem. Soc. Jpn.* **1994**, *67*, 1598–1607.
- [11] a) R. Breslow, B. Zhang, *J. Am. Chem. Soc.* **1996**, *118*, 8495–8496; b) R. Breslow, S. Chung, *J. Am. Chem. Soc.* **1990**, *112*, 9659–9660; c) R. Breslow, N. Greenspoon, T. Guo, R. Zarzycki, *J. Am. Chem. Soc.* **1989**, *111*, 8296–8297.
- [12] a) W. D. Kohn, C. M. Kay, B. D. Sykes, R. S. Hodges, *J. Am. Chem. Soc.* **1998**, *120*, 1124–1132; b) N. E. Zhou, C. M. Kay, B. D. Sykes, R. S. Hodges, *Biochemistry* **1993**, *32*, 6190–6197.
- [13] a) K. R. Shoemaker, P. S. Kim, E. J. York, J. M. Stewart, R. L. Baldwin, *Nature (London)* **1987**, *326*, 563–567; b) K. R. Shoemaker, P. S. Kim, D. N. Brems, S. Marqusee, E. J. York, I. M. Chaiken, J. M. Stewart, R. L. Baldwin, *Proc. Natl. Acad. Sci. USA* **1985**, *82*, 2349–2353; c) P. B. Harbury, T. Zhang, P. S. Kim, R. L. Baldwin, *Science* **1993**, *262*, 1401–1407; d) G. Merutka, W. Shalongo, E. Stellwagen, *Biochemistry* **1991**, *30*, 4245–4248.
- [14] a) M. Allert, M. Kjellstrand, K. Broo, Å. Nilsson, L. Baltzer, *Chem. Commun.* **1998**, 1547–1548; b) K. S. Broo, H. Nilsson, J. Nilsson, L. Baltzer, *J. Am. Chem. Soc.* **1998**, *120*, 10287–10295.
- [15] a) R. B. Hill, W. F. DeGrado, *J. Am. Chem. Soc.* **1998**, *120*, 1138–1145; b) S. T. R. Walsh, H. Cheng, J. W. Bryson, H. Roder, W. F. DeGrado, *Proc. Natl. Acad. Sci. USA* **1999**, *96*, 5486–5491.
- [16] R. Corradini, A. Dossena, R. Marchelli, A. Panagia, G. Sartor, M. Saviano, A. Lombardi, V. Pavone, *Chem. Eur. J.* **1996**, *2*, 373–381.
- [17] R. A. Dunbar, F. V. Bright, *Supramol. Chem.* **1994**, *3*, 93–99.
- [18] S. Marqusee, R. L. Baldwin, *Proc. Natl. Acad. Sci. USA* **1987**, *84*, 8898–8902.
- [19] S.-H. Park, W. Shalongo, E. Stellwagen, *Biochemistry* **1993**, *32*, 12901–12905.
- [20] T. Morii, J. Yamane, Y. Aizawa, K. Makino, Y. Sugiura, *J. Am. Chem. Soc.* **1996**, *118*, 10011–10017.
- [21] a) N. Kobayashi, S. Minato, T. Osa, *Macromol. Chem.* **1983**, *184*, 2123–2132; b) N. Kobayashi, R. Saito, H. Hino, Y. Hino, A. Ueno, T. Osa, *J. Chem. Soc. Perkin. Trans. 2*, **1983**, 1031–1035.
- [22] a) K. Harata, H. Uedaira, *Bull. Chem. Soc. Jpn.* **1975**, *48*, 375–378; b) K. Harata, *Bull. Chem. Soc. Jpn.* **1978**, *51*, 2737–2738; c) H. Shimizu, A. Kaito, M. Hatano, *Bull. Chem. Soc. Jpn.* **1979**, *52*, 2678–2684.
- [23] a) M. Kodaka, *J. Phys. Chem.* **1991**, *95*, 2110–2112; b) M. Kodaka, *J. Am. Chem. Soc.* **1993**, *115*, 3702–3705.
- [24] a) M. Kitagawa, H. Hoshi, M. Sakurai, Y. Inoue, R. Chûjô, *Bull. Chem. Soc. Jpn.* **1988**, *61*, 4225–4229; b) M. Sakurai, M. Kitagawa, H. Hoshi, Y. Inoue, R. Chûjô, *Carbohydr. Res.* **1990**, *198*, 181–191; c) A. Botsi, K. Yannakopoulou, E. Hadjoudis, J. Waite, *Carbohydr. Res.* **1996**, *283*, 1–16.
- [25] a) R. F. Chen, *Arch. Biochem. Biophys.* **1967**, *120*, 609–620; b) J. B. Bridge, P. Johnson, *Eur. Polym. J.* **1973**, *9*, 1327–1346.
- [26] F. V. Bright, G. C. Catena, J. Huang, *J. Am. Chem. Soc.* **1990**, *112*, 1343–1346.
- [27] a) R. Wang, F. V. Bright, *Appl. Spectrosc.* **1993**, *46*, 792–799; b) R. Wang, F. V. Bright, *Appl. Spectrosc.* **1993**, *46*, 800–806.
- [28] a) B. R. Gibney, F. Rabanal, J. J. Skalicky, A. J. Wand, P. L. Dutton, *J. Am. Chem. Soc.* **1999**, *121*, 4952–4960; b) J. K. Myers, C. N. Pace, J. M. Scholtz, *Protein Sci.* **1995**, *4*, 2138–2148.
- [29] E. Atherton, R. C. Sheppard, *Solid Phase Peptide Synthesis: A Practical Approach*, IRL Press, Oxford, **1989**.
- [30] H. Rink, *Tetrahedron Lett.* **1987**, *28*, 3787–3790.
- [31] E. Kaiser, R. L. Collescott, C. D. Bossinger, *Anal. Biochem.* **1970**, *34*, 595–598.
- [32] N. Fujii, A. Otaka, O. Ikemura, K. Akagi, S. Funakoshi, Y. Hayashi, Y. Kuroda, H. Yajima, *J. Chem. Soc. Chem. Commun.* **1987**, 274–275.

Received: September 13, 1999 [F2030]